

Reflection of Radio Waves From Undulating Tropospheric Layers¹

A. T. Waterman, Jr., and J. W. Strohbehn

Contribution from Systems Techniques Laboratory, Stanford Electronics Laboratories,
Stanford University, Stanford, Calif.

(Received June 28, 1963)

This report examines the nature of coherent reflections of radio waves, at near-grazing incidence, from a horizontal atmospheric layer on which is superimposed a slight wave motion. The existence of reflections of this type is merely postulated, and the development then proceeds to examine the consequences of such a postulate with reference to measurements obtainable in transhorizon propagation experiments. The properties of angle of arrival, signal level, fading rate, and Doppler shift are examined, together with their rates of change with time.

1. Introduction

Certain rapid beam-swinging experiments in transhorizon microwave propagation have been reported [Waterman, 1958] as showing an apparently systematic motion of the scattering or reflecting source with velocities in excess of wind speed. The suggestion that these motions might be associated with waves² on a surface of discontinuity in refractive index [Waterman, 1959] has been examined by Gossard [1961; 1962] who concluded, on meteorological grounds, that the wave velocities were incompatible with the angles, slopes, and refractive-index discontinuities required.

This report examines the nature of such hypothesized reflections with regard to the angle of arrival, signal strength, Doppler shift, and fading rates of the received signal. It is shown that the location of a reflecting facet on a wavy layer does not move with the phase velocity of the wave; in fact, it can move in the opposite direction, and can have infinite velocity. From a single sinusoidal layer and at a given instant of time, there may exist one, three, or more distinct rays leading to multipath phenomena. The variation in signal strength, for the case of a single ray, is caused by changes in the angle of incidence and by focusing of the energy by the layer's curvature. The Doppler is caused by the motion of the reflecting point, both in elevation and in azimuth. The effects on the signal strength of multiple layers at different elevations are considered. For a number of these structures, various signal statistics—distribution, power spectrum, time autocorrelation—are computed. The main purpose is to evolve a theoretical basis for comparing predicted results of radio reflections from layers with experimental measurements.

2. Geometry of Layer Reflections

In most transhorizon propagation paths the scattering or reflecting regions occur near the center of the path. If off-path reflections from a layer occur, the layer must have an appropriately oriented slope. For simplicity of analysis, we consider waves moving at right angles to the path and reflection from a facet on the midplane between transmitter and receiver. The facet's position is then specified by an azimuth a , and an elevation e , as seen by the receiver. In order that a ray from the transmitter be specularly reflected in the direction of the receiver, the slope of the facet must be given by

$$\tan S_r = -\frac{\tan a \cdot \cos e}{\sin \left(e + \frac{D}{2R} \right)} \approx -\frac{a}{e + \frac{D}{2R}} \quad (1)$$

in which D is the path length and R is the earth's radius. The approximation is valid since the angles are small. This is the slope necessary for reflection, so designated by the subscript r . It must be equated to an expression for the slope of the layer. Consider a sinusoidal wave with vertical displacement z , amplitude A , and wavelength L , traveling in the x direction, normal to the path. It may be represented by

$$z = H + A \cos \left(\Omega t - \frac{2\pi x}{L} \right) \quad (2)$$

and its slope is equal to

$$\begin{aligned} \tan S_l &= \frac{dz}{dx} = \left[\frac{2\pi A}{L} \sin \left(\Omega t - \frac{2\pi x}{L} \right) \right] \\ &\approx +\frac{2\pi A}{L} \sin \left(\Omega t - \frac{\pi D}{L} a \right) \end{aligned} \quad (3)$$

¹ Prepared under Signal Corps Contract DA 36-039 SC-87300.

² With regard to the existence of such waves, see: [Gossard 1954, Smyth, 1947 and du Castel, 1961].

if the lateral distance x is replaced by $Da/2$. (The subscript l indicates that this is the layer slope which must be equated to $\tan S_r$ above.) Therefore, at the reflecting point, we must have

$$-\frac{a}{e + \frac{D}{2R}} = \frac{2\pi A}{L} \sin\left(\Omega t - \frac{\pi Da}{L}\right). \quad (4)$$

For a given path, specified by D , and a given wavy layer, specified by A , L , Ω , and e , a solution of this equation for a will determine the azimuth from which reflections may be obtained. As time t varies, the waves move along the layer and the value of azimuth a varies.

The nature of this variation may be seen by solving (4) graphically. Figure 1 illustrates the situation in two sample cases. The slope required for reflection varies linearly with azimuth—eq. (1)—and is indicated by the oblique straight line in the upper diagram. The slope of a relatively flat sinusoidal layer is indicated by the dashed line. Where these two lines intersect, the azimuth of the reflecting point is specified—i.e., (4) is satisfied. As this flat sinusoidal layer moves across the path, the position of the intersection varies, but there is never

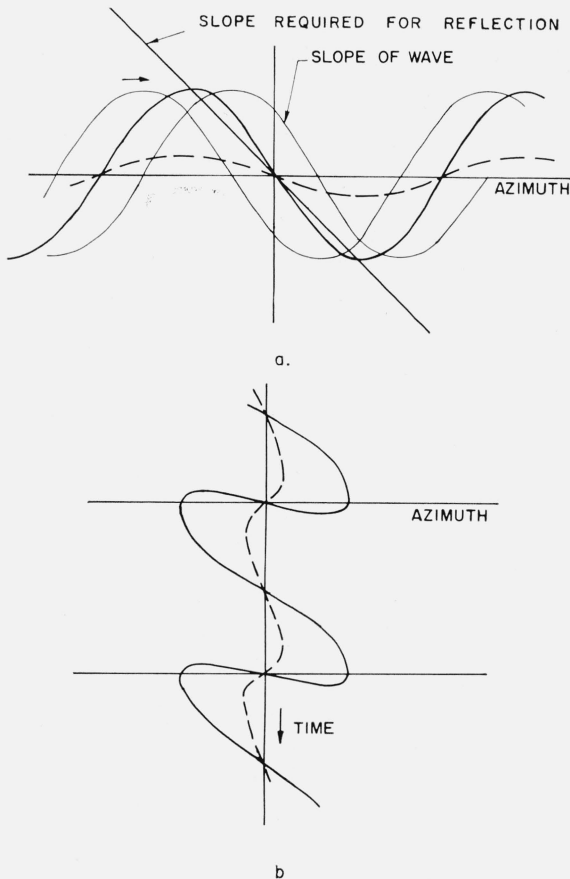


FIGURE 1. Graphical method of solution for azimuthal position of reflecting point from a sinusoidal wavy layer.

more than one intersection and consequently never more than one reflection. The azimuth of the reflection wanders back and forth in a distorted sinusoidal motion.

A more pronounced sinusoid, having steeper slopes, is indicated by the solid wave in the upper diagram of figure 1. Three positions are shown as it moves across the path. In one of these, there are three intersections with the oblique straight line and consequently three reflecting points on one layer. The lower part of the figure has the same azimuth scale, but time runs vertically downward. The dashed and solid curves indicate the motion of the reflecting point as seen by the receiver for the two cases of a flat and steep sinusoidal wave. For the latter wave, the time interval during which three reflections are possible is evident: as one reflection moves off to the side in azimuth another appears and immediately splits into two reflections, one of which swings across the great-circle bearing (zero azimuth) and joins the first, where they both disappear, while the other swings out to a maximum azimuth and then returns more slowly.

In this figure the rate of change of azimuth with time is given by the slope with respect to the vertical time scale. Where the curves have a vertical tangent, the azimuthal velocity is zero; where horizontal, infinite. Thus the coming and going of the multiple reflections are accompanied by momentarily infinite velocities.

It is convenient to classify wavy layers in accordance with the magnitude of the maximum facet velocity. For the cases considered here (small sinusoidal waves on horizontal layers and moving across the path), a parameter η may be defined whose properties are: (1) it is zero for a completely flat layer, (2) it equals 0.5 for a layer whose maximum facet velocity equals the wave velocity, and (3) it equals unity for a layer of just sufficient slope to support infinite facet velocities. This parameter is related to the layer and path geometry by

$$\eta = \frac{2\pi A}{L} \cdot \frac{\pi D}{L} \cdot \left(e + \frac{D}{2R}\right) \quad (5)$$

- $\eta=0$: facet velocity less than wave velocity
- $\eta=0.5$: maximum facet velocity equals wave velocity
- $\eta=1.0$: maximum facet velocity infinite; three or more reflections per layer.

We may now define waves on a layer as *small* if $\eta < 0.5$, and as *large* if $\eta \geq 1.0$.

An indication of the variations in the angular velocity of the reflecting facet can be seen from figure 2, in which azimuth is plotted as a function of time for three pairs of different geometrical cases. In these cases the amplitude and wavelength of each layer have been held constant, while the distance has been doubled between Case I and Case II, and again between Case II and Case III. In each case, two layer elevations are considered, the lower being represented by the dashed curve.

Examining Case I we see that at both elevations

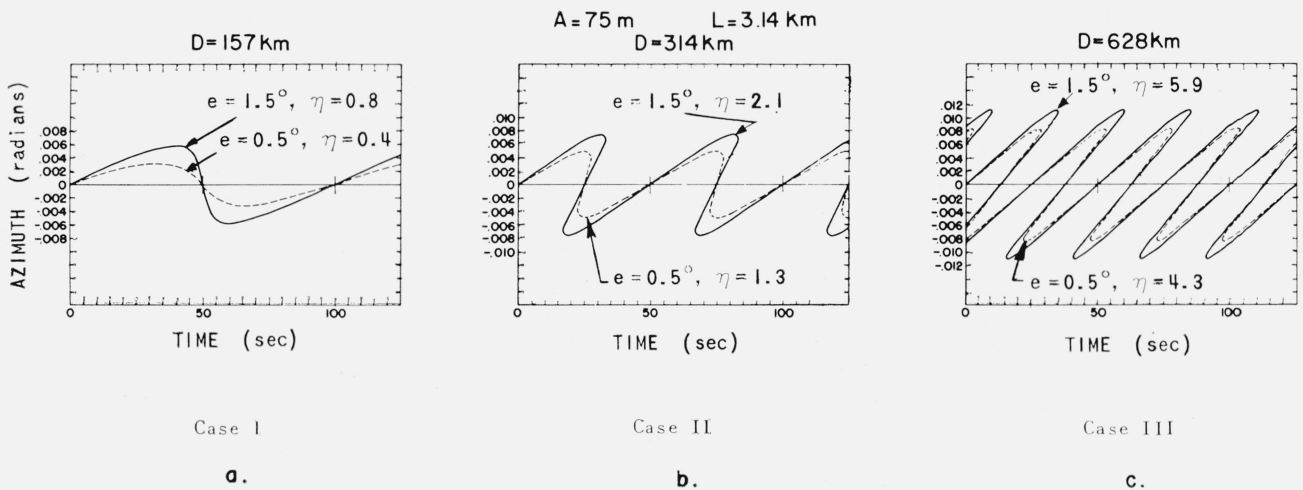


FIGURE 2. Angle of arrival for rays reflected from a wavy layer of form $H + A \cos\left(\Omega t - \frac{2\pi x}{L}\right)$.

the facet velocity never becomes infinite. For these two curves the parameter η is approximately 0.4 and 0.8 for the elevation angles of 0.5 deg and 1.5 deg respectively. This means that for the lower elevation the maximum facet velocity is approximately equal to the wave velocity. However, it is in the opposite direction; the wave is moving from negative to positive azimuths, while the maximum rate of change of facet azimuth occurs in going from positive to negative (at $t=50$ sec, in the figure). For the higher elevation we have a much steeper slope in the region near zero azimuth corresponding to a high angular velocity of the received ray.

In Cases II and III, with the increased distances η has become larger than 1.0. As a result we have some momentarily infinite velocities and more than one reflecting point. The second case shows as many as three received rays during part of the cycle, and the third case shows as many as five with never fewer than three.

Figure 2 illustrates the effects that changing the distance between transmitter and receiver can have on the characteristics of the received signal from a given layer. As the distance is increased, the angular velocity of the reflecting facet will increase until its peak value equals that of the wave; as distance is increased further, the peak facet velocity will eventually become infinite and more than one ray will be received. Similar effects would be observed for a progressive increase in layer elevation or in wave amplitude, or for a decrease in wavelength.

3. Signal Strength

While there are several factors affecting signal strength, we discuss here only some elementary considerations directly related to the hypothesis of layer reflections. First is the magnitude of the reflection coefficient for a plane (nonwavy) layer. If the "layer" consists of an abrupt change in refractive index Δn from a uniform value below to a different

uniform value above, the power reflection coefficient is

$$\rho = \left(\frac{2\Delta n}{\theta^2}\right)^2 \quad (6)$$

where θ is twice the angle between the plane of the interface and the wave normal—i.e., the total deviation angle of the reflected wave. Computations have been made of the reflection coefficient [Bauer, 1956] for cases in which the discontinuity is not abrupt but is distributed over a distance that is not a small fraction of a wavelength. In many reasonable cases these computed reflection coefficients do not differ markedly from that in (6), and so it will be used for purposes of discussion. The magnitude of the signal reflected from a layer, then, will vary with layer height, other quantities remaining unaltered. Indeed it is interesting to note that the power reflection coefficient varies inversely as the fourth power of the deviation angle θ . This dependence is similar to that predicted from the quite different model of turbulent blobs [Booker and Gordon, 1950]. As regards magnitude, a discontinuity of one N unit in refractive index (one part in 10^6) and a deviation angle of 2 deg give rise to a reflected wave about 55 db below the incident, a figure which is comparable with both turbulent-model predictions and experimental observations.

Another effect on signal strength must also be taken into account: the focusing factor. Since the layer is curved, the reflected rays may diverge less strongly or more strongly than in the absence of layer curvature. For instance, consider the layer previously mentioned. At time $t=0$, reflection takes place on the great-circle plane, and since the layer is concave downward, the reflected wave is focused toward the receiver, resulting in a higher signal strength than for a flat layer with the same discontinuity. Defining the focusing factor as a ratio of the received power after reflection from a curved layer to the received power after reflection from a

$A = 75 \text{ m}$
 $L = 3.14 \text{ km}$
 $D = 157 \text{ km}$
 $v = 31.4 \text{ m/sec}$

$A = 137.5 \text{ m}$
 $L = 3.14 \text{ km}$
 $D = 157 \text{ km}$
 $v = 31.4 \text{ m/sec}$

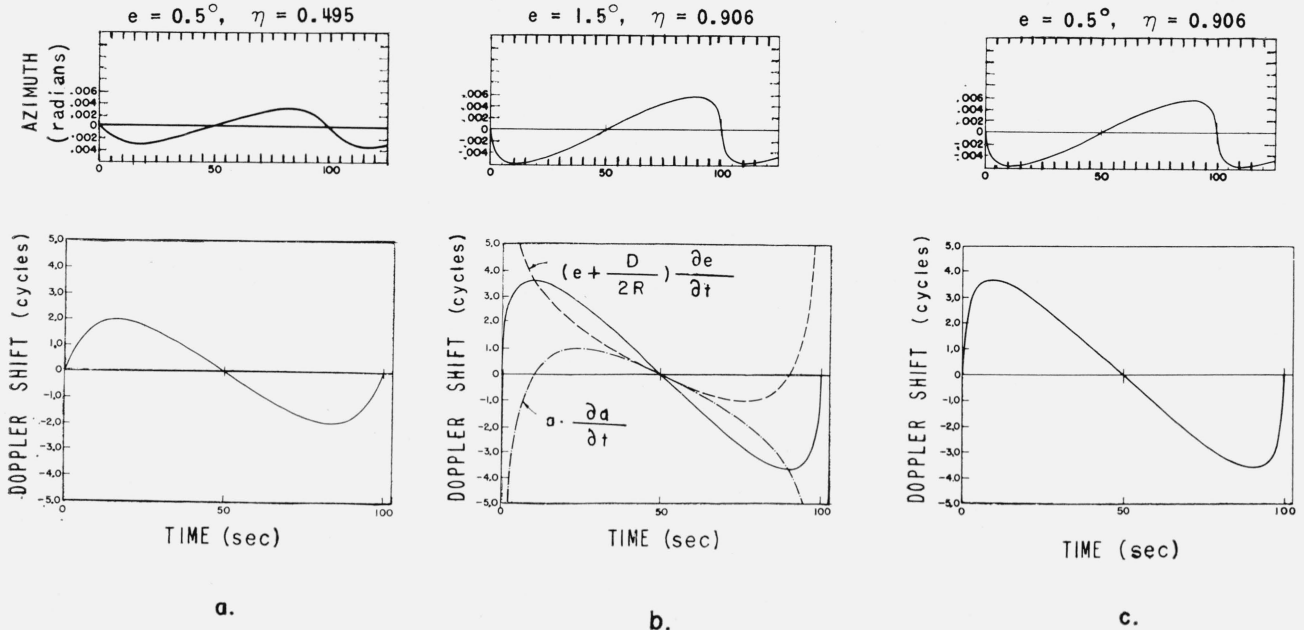


FIGURE 4. Angle of arrival and Doppler shift as functions of time for wavy layers with a single reflecting point.

Presumably, slight departures from the idealized model assumed here could permit either term to predominate. Hence, rapid changes in Doppler at these moments are possible.

5. Several Layers With a Single Reflecting Point

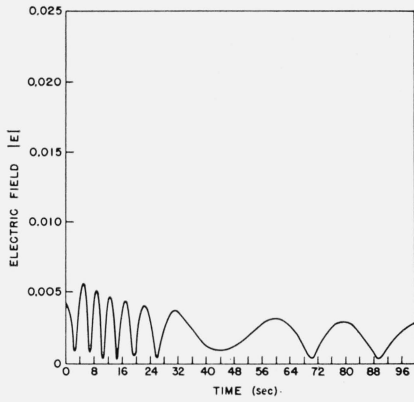
When more than one layer is present, the curves for received signal strength are no longer as well-behaved as in figure 3. In figures 5 and 6 we have assumed two wavy layers—and in figures 7 and 8, three wavy layers—each supporting a single ray. In all of these cases we have assumed that the wavy layers are identical in shape but are at different elevations. On each figure we have shown not only the signal strength, but also the amplitude distribution and the power spectrum.

Plots of typical signal strength (electric field) versus time are shown in figures 5a to 8a. The rapid variations observed in these figures result from the beating between the two or three received rays. The beating results from the change in path lengths associated with different azimuth positions of the reflected ray. In figure 5a the two layers are at nearly the same height (around 1 deg above the horizon), and consequently both reflected rays are nearly equal in amplitude so that the interference fades are deep and relatively slow. However, in figure 6a the layers are farther apart (one at 0 deg, the other at 0.75 deg elevation) so that the reflection closer to grazing is appreciably stronger; the interference fades are therefore less pronounced, but the fading rate is

markedly increased. In figures 7a and 8a, the addition of a third layer has made the received signal more erratic. The only difference between these two figures is the position of the middle layer. The fades are deeper if the middle layer is close to the lower layer (fig. 8), since the lower one has the strongest amplitude; but when the middle layer is close to the top one, the fading rate is seen to be more rapid.

In figures 5b to 8b the signal distribution is plotted on a Rayleigh scale. On this scale a Rayleigh distribution has a negative 45-deg slope as shown by the dashed curve. In figures 5 and 8 the distributions roughly approximate a Rayleigh distribution—even though the signal is made up of two and three components respectively—and the phase relations are deterministic rather than random. In figures 7 the distribution is a close approximation to a Rice distribution [Rice, 1945; Beckmann, 1961] which is the sum of a constant vector plus a Rayleigh distributed vector. As has been noted previously for other circumstances, one finds that the distribution of a signal resulting from a small number of components can often approximate more complicated distributions.

In figures 5c to 8c we have plotted the power spectrum. The spectrum was obtained by computing the time autocorrelation and then taking the Fourier transform to find the power spectrum. A hanning window was used [Blackman and Tukey, 1958]. Though in most cases the power spectrum peaks up at only one or two frequencies, in figure 7 quite a broad spectrum is observed.

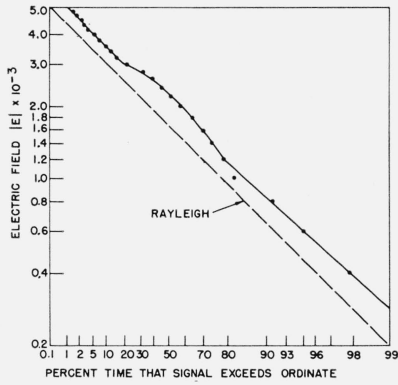


DIMENSIONS OF WAVY LAYERS:

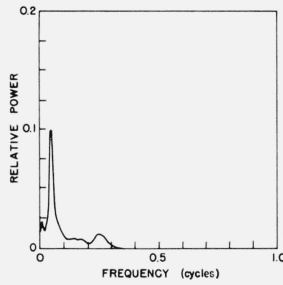
	I	II
AMPLITUDE (m)	49.2	49.2
LENGTH (m)	3142	3142
ELEVATION (deg)	1	1.1
η	0.477	0.504

DISTANCE TO TRANSMITTER (m): 160,935
 RADIO WAVELENGTH (m): 0.1

a. Magnitude of electric field $|E|$ vs time t .

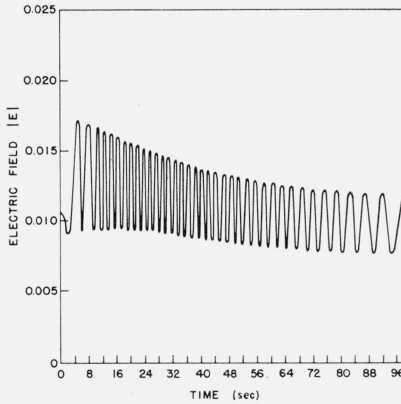


b. Distribution of signal levels.



c. Power spectrum.

FIGURE 5. Properties of received signal reflected from two layers that are close together.

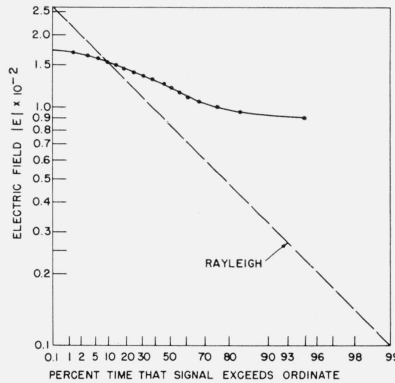


DIMENSIONS OF WAVY LAYERS:

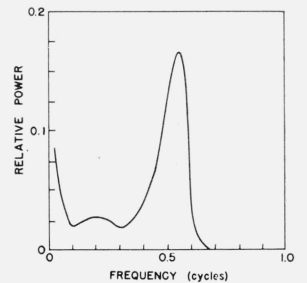
	I	II
AMPLITUDE (m)	75	75
LENGTH (m)	3142	3142
ELEVATION (deg)	0	0.75
η	0.305	0.620

DISTANCE TO TRANSMITTER (m): 160,935
 RADIO WAVELENGTH (m): 0.1

a. Magnitude of electric field $|E|$ vs time t .

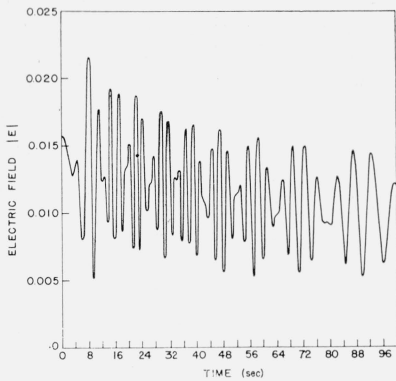


b. Distribution of signal levels.



c. Power spectrum.

FIGURE 6. Properties of received signal reflected from two layers that are far apart.

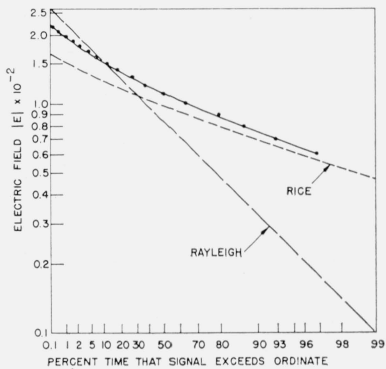


DIMENSIONS OF WAVY LAYERS:

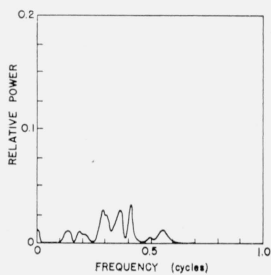
	I	II	III
AMPLITUDE (m)	75	75	75
LENGTH (m)	3142	3142	3142
ELEVATION (deg)	0	0.573	0.75
η	0.305	0.546	0.620

DISTANCE TO TRANSMITTER (m): 160,935
 RADIO WAVELENGTH (m): 0.1

a. Magnitude of electric field $|E|$ vs time t .

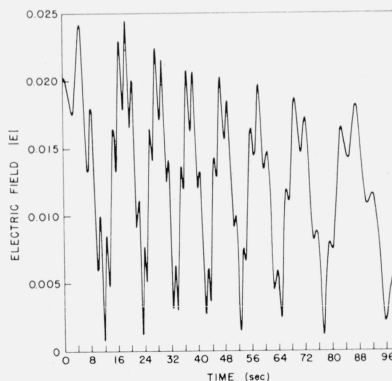


b. Distribution of signal levels.



c. Power spectrum.

FIGURE 7. Properties of received signal reflected from three layers (two with high elevation).



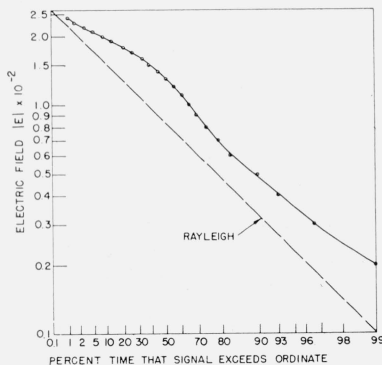
DIMENSIONS OF WAVY LAYERS:

	I	II	III
AMPLITUDE (m)	75	75	75
LENGTH (m)	3142	3142	3142
ELEVATION (deg)	0	0.15	0.75
η	0.305	0.367	0.620

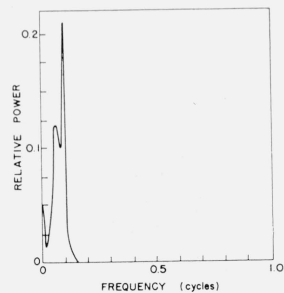
DISTANCE TO TRANSMITTER (m): 160,935
 RADIO WAVELENGTH (m): 0.1

FIGURE 8. Properties of received signal reflected from three layers (two with low elevation).

a. Magnitude of electric field $|E|$ vs time t .



b. Distribution of signal levels.



c. Power spectrum.

6. Wavy Layers With More Than One Reflecting Point

In figure 2 there are two cases where a single layer supports more than one reflected ray during at least part of the time ($\eta > 1$). Just as in the case of multiple layers, there is a beat between the several rays. An example of this effect is seen in figure 9 for the layer shown in the second case of figure 2. Only a detailed portion of the time record is shown, starting just before the wave moves from the position in which it supports one reflection to the position in which it supports three. With the onset of three reflections, rapid fading commences. It is faster—because of the rapid motions of the reflecting facets during this part of the cycle—than the fading associated with multiple, relatively flat ($\eta < 1$) layers. However, this rapid fading occurs only when there are several rays present. The rest of the time the signal is quite steady. As mentioned earlier, the maximum slopes of the wavy layers must exceed a critical value before such rapid fading will occur.

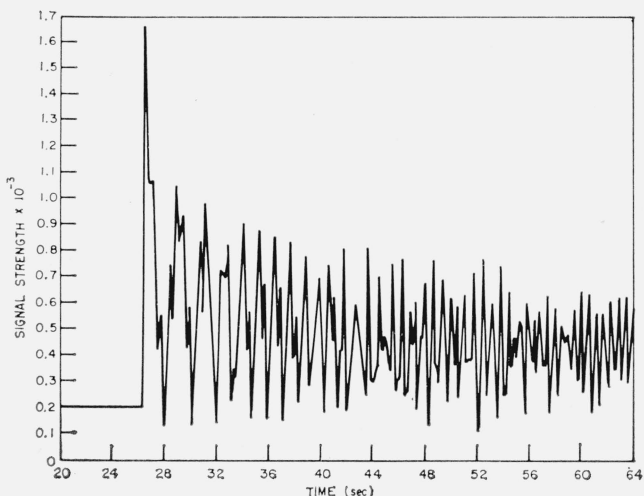


FIGURE 9. Rapid fading due to three rays received from a single layer.

7. Conclusion

We have examined quantitatively the consequences of an atmospheric model consisting of low-amplitude waves on a nearly horizontal surface of discontinuity—or abrupt change—in refractive index. The model is assumed to be one deserving consideration as a mechanism for transhorizon propagation, and the results derived relate to phenomena which may be observed in transhorizon experiments. Specifically, we have evaluated the azimuth of arrival and its time rate of change, the signal level and its variation, the Doppler shift, and the received-signal distribution and power spectrum. We have investigated so far a variety of single-layer and multiple-layer conditions.

The azimuthal deviations from a great-circle trajectory are strongly dependent on layer elevation as well as wave slope on the layer. Rate of change of azimuth is critically dependent on a parameter

η which is proportional to maximum wave slope and to layer elevation. For layers such that $\eta > 0.5$, the velocity of the reflecting point on the layer may exceed the wave velocity; and for $\eta > 1$, multiple reflections from one layer may exist and their motions may have momentarily infinite velocities. Signal levels are influenced not only by the magnitude of the discontinuity and the grazing angle (in a manner very similar to that predicted by turbulent scattering), but also by layer curvature imparted by the wave. The consequent focusing results in signal peaks (of several decibels) coincident with the moments of fastest azimuth variation. Doppler shifts of a few cycles per second are likely—at 3 Gc/s for a 100-mile path—and are proportional to radio-frequency and to the first or second power of path length. These shifts change most rapidly at the moments of fast azimuth motion and signal peaking. The presence of more than one layer may lead to rapid fading: when two or more of the strongest reflections are nearly equal, the resulting signal-level distribution is approximately Rayleigh; and if one reflection predominates, it resembles a Rice distribution. Under some circumstances, particularly for a layer whose maximum slope just exceeds the critical value ($\eta > 1$), the fading may change abruptly, jumping to much higher rates during a small portion of the cycle. It is interesting to note that this type of phenomenon is similar to that attributed to the passage of an airplane across the transmission path.

8. References

- Bauer, J. R. (Sept. 24, 1956), The suggested role of stratified elevated layers in transhorizon short-wave radio propagation, Tech. Rept. No. 124, Lincoln Laboratory, M.I.T., Cambridge, Mass.
- Beckmann, P. (1961), The statistical distribution of the amplitude and phase of a multiply scattered field, Inst. Radio Eng. and Electron., Czech. Acad. Sci. **18**, 41.
- Blackman, R. B., and J. W. Tukey (1958), The measurement of power spectra, pp. 14-15 (Dover Publications, Inc., New York, N.Y.).
- Booker, H. G., and W. E. Gordon (Apr. 1950), A theory on radio scattering in the troposphere, Proc. IRE **38**, 401.
- Gossard, E. E. (Aug. 1954), On gravity waves in the atmosphere, J. Meteorol. **II**, 259-269.
- Gossard, E. E. (May 3, 1961), Internal waves on a refractive layer and their effect on tropospheric propagation, URSI Meeting, Washington, D.C.
- Gossard, E. E. (May 3, 1962), The reflection of microwaves by a refractive layer perturbed by waves, Trans. IRE Ant. Prop. **AP-10**.
- Rice, S. O. (1944), Mathematical analysis of random noise, Bell Syst. Tech. J. **23**, 282-332.
- Rice, S. O. (1945), Mathematical analysis of random noise, Bell Syst. Tech. J. **23**, 46-156.
- Waterman, A. T., Jr. (Apr. 26, 1958), A rapid beam-swinging experiment, URSI Meeting, Washington, D.C.
- Waterman, A. T., Jr. (Oct. 1958), A rapid beam-swinging experiment, IRE Trans. Ant. Prop. **AP-5**, 338.
- Waterman, A. T., Jr. (May 6, 1959), The mechanism of transhorizon propagation: layers vs turbulence, URSI Meeting, Washington, D.C.

Additional References

- duCastel, F. (1961), Propagation tropospherique et Faisceaux Hertzien Transhorizon, Editions Chiron, Paris, pp. 56-63.
- Smyth, J. B., and L. G. Trolese (1947), Propagation of radio waves in the lower troposphere, Proc. IRE **35**, 1198. (Paper 67D6-294)